LAWRENCE
LIVERMORE
NATIONAL
LABORATORY

LLNL-PROC-753558

Developing Accurate Semi-Empirical Quantum Models for CNHO Chemistry at Detonation Conditions

M. P. Kroonblawd, N. Goldman, R. K. Lindsey

June 22, 2018

16th International Detonation Symposium
Cambridge, MD, United States
July 15, 2018 through July 20, 2018

Disclaimer

Developing Accurate Semi-Empirical Quantum Models for CNHO Chemistry at Detonation Conditions

Matthew P. Kroonblawd[†], Nir Goldman[†,‡], and Rebecca K. Lindsey[†]

[†]Lawrence Livermore National Laboratory, Livermore, CA 94550, USA
[‡]Department of Chemical Engineering, University of California, Davis, CA 95616, USA

Abstract. We describe two approaches to develop accurate models for CNHO chemistry through force matching comparatively inexpensive semi-empirical quantum models to *ab initio* data. The approaches used to generate *ab initio* training data differ depending on the kinetics for the chemistry of interest and are applied to aqueous glycine chemistry under ambient and detonation-like conditions. Significant correlations between potential energy functions parameterized using both approaches are noted and possible implications for model development are discussed. A force-matched model is applied to predict glycine chemistry under detonation-like conditions.

Introduction

Quantum-based molecular dynamics (QMD) simulations are critical for predicting chemistry and can help guide the design and interpretation of expensive experiments. First principles approaches based on density functional theory[1] (DFT) are highly accurate, but their extreme computational cost typically imposes harsh limits on the accessible space and time scales (often reaching only nanometers and picoseconds). Semi-empirical approaches such as density functional tight binding[2] (DFTB) hold promise to retain DFT-level accuracy and afford up to a thousand-fold reduction in computational cost. DFTB with self-consistent charges is capable of modeling organic chemistry because it captures bond formation/dissociation and charge transfer. Moreover, because DFTB is derived from DFT, it is generally more accurate and transferable than classical reactive force fields. Off-the-shelf DFTB models can be inaccurate in their description of chemistry (especially at extreme conditions),[3, 4, 5, 6] but are highly amenable to tuning for specific systems.[5, 6, 7, 8] In this report, we describe two general approaches to parameterize DFTB models for reactive CNHO systems based on force matching. The approaches differ depending on the kinetics for the chemistry of interest, ranging from fast reactions that occur within picoseconds[5] to situations with large barriers that prevent direct QMD simulation.[6]

Self-consistent charge DFTB is derived[2] from an expansion of the Kohn-Sham energy to second order in charge fluctuations. The total DFTB energy,

$$E_{\mathrm{DFTB}} = E_{\mathrm{BS}} + E_{\mathrm{Coul}} + E_{\mathrm{Rep}}, \quad (1)$$

is separated into contributions from the electronic band structure (E_{BS}), Coulombic interactions between the fluctuating partial charges (E_{Coul}), and an empirical repulsive potential (E_{Rep}) that accounts for ionic repulsion and Kohn-Sham double counting terms. Generic parameter sets usually fit E_{Rep}

to reproduce energies and/or forces for gas phase molecules.[2, 9] In contrast, we explore fitting E_{Rep} to DFT force data obtained for configurations extracted during condensed-phase chemical reactions through the force matching method.[10, 11] As in previous work,[5, 6, 7] we define E_{Rep} as a set of pairwise interactions expressed as a power series,

$$E_{\mathrm{Rep}}^{\alpha\beta} = \begin{cases} \sum_{n=2}^{9} c_n^{\alpha\beta}(r_{\mathrm{c}}^{\alpha\beta} - r_{ij})^n & r_{ij} \leq r_{\mathrm{c}}^{\alpha\beta} \\ 0 & \text{otherwise,} \end{cases} \quad (2)$$

that is linear in its coefficients $c_n^{\alpha\beta}$. Here, r_{ij} is the separation distance between atom i of type α and j of type β and $r_{\mathrm{c}}^{\alpha\beta}$ is a distance cutoff that is typically $\approx$2 Å. Because Eq. 2 is linear in $c_n^{\alpha\beta}$, the coefficients can be fit rapidly using techniques such as singular value decomposition. Specifically, we find the set of $c_n^{\alpha\beta}$ that minimize the root mean-square error (RMSE) in the forces $\mathbf{F}_{\mathrm{Rep}}^*$ attributed to the repulsive interactions,

$$\mathrm{RMSE} = \sqrt{\frac{1}{3NQ}\sum_q \left(\mathbf{F}_{\mathrm{Rep},q}^* - \mathbf{F}_{\mathrm{Rep},q}\right)}. \quad (3)$$

Here, the target repulsive forces are computed as

$$\mathbf{F}_{\mathrm{Rep}}^* = \mathbf{F}_{\mathrm{DFT}} - \mathbf{F}_{\mathrm{BS}} - \mathbf{F}_{\mathrm{Coul}}, \quad (4)$$

where $\mathbf{F}_{\mathrm{DFT}}$ is the force predicted by DFT and $\mathbf{F}_{\mathrm{BS}}$ and $\mathbf{F}_{\mathrm{Coul}}$ are the DFTB forces from the band structure and Coulombic energy contributions that are treated as pre-determined. The sum runs over the Q configurations indexed by q and each force vector is of length $3N$, where N is the number of atoms. A primary difficulty in the development of a force-matched DFTB model is in constructing a suitable DFT training set for particular reactions or reaction conditions.

When the chemistry of interest is fast relative to practical DFT simulation times (typically 10 – 100 ps, depending on simulation parameter choices), important configurations for force matching can be sampled directly through standard DFT-based QMD.[5] Extreme temperature and pressure conditions, such as those realized during a detonation or impact event, often facilitate rapid chemistry (see, for instance Refs. 5, 12, and 13). However, such conditions can also facilitate accessing many reaction paths that cannot be sampled by a single simulation.[12] In this case, relatively short timescale DFT simulations can be used to train DFTB models that efficiently reach longer times and are inexpensive enough to run in ensembles of independent simulations.

In situations where reaction barriers are more than a few $k_{\mathrm{B}}T$, the reactive processes of interest are often too slow or rare to sample directly with standard QMD based on either DFT or DFTB. One approach to accelerate the sampling of reactive events is to apply a bias potential to one or more collective coordinates that distinguish between reactants and products and describe the reaction path.[13, 14, 15, 16] Bias potentials drive the system over energetic barriers to explore important phase space configurations for force matching that have a high relative free energy compared to the reactants and products at equilibrium.[6, 17] Free energy landscapes can be extracted from biased simulations, with the particular extraction approach determined by the manner in which the bias was applied (*e.g.*, metadynamics[13] or umbrella sampling[18, 19]).

We develop and apply force-matched DFTB models to predict glycine chemistry under different prebiotic conditions. Two scenarios are considered with different inherent timescales for chemical reactivity. In Approach 1, we force match a DFTB model to a 1:1 water:glycine mixture under cometary impact conditions ($T = 3000$ K, $P = 50$ GPa) with rapidly evolving chemistry. DFTB is used to significantly extend the simulation time to model chemistry during the adiabatic expansion and cooling of small ejected cometary fragments. In Approach 2, we force match a distinctly different DFTB model to slow aqueous glycine condensation reactions at ($T = 300$ K, $P = 0$ GPa) using umbrella sampling to simultaneously generate training data and estimate the reaction free energy surface. Approach 2 and the corresponding glycine DFTB model were first developed in Ref. 6, wherein it was found that multiple nanoseconds of DFTB trajectory were needed to converge free energy predictions. Similarities in the two force-matched DFTB models are described. Both approaches are fully generalized for CNHO systems and can be readily extended to model detonation chemistry of other organic materials.

Methods

All DFTB simulations were performed using the Large-scale Atomic/Molecular Massively Parallel Simulator[20] (LAMMPS) with forces and stresses evaluated by the DFTB+ code.[21] Trajectories were integrated using Extended Lagrangian Born-Oppenheimer dynamics[22, 23] with a 0.2 fs time step. The electronic structure was evaluated without spin polarization at the Γ point only using four self-consistent charge cycles per time step and with Fermi-Dirac thermal smearing where the electronic temperature was set equal to the ionic temperature at each time step. Isothermal-isochoric (*NVT*) simulations were performed using a Nosé-Hoover-style thermostat.[24, 25] The mio-1-1 DFTB parameter set (available at http://www.dftb.org), a typical off-the-shelf parameterization for organic systems, was used for all calculations. Selected generic E_{Rep} potentials from mio-1-1 were replaced with force-matched potentials specifically noted below.

Two different plane-wave DFT codes were used for the DFT simulations due to code-linking requirements. All DFT simulations used the Perdew-Burke-Ernzerhof[26] (PBE) generalized gradient approximation functional with electronic structure evaluations performed without spin polarization at the Γ point only. Simulations sampling fast chemistry (Approach 1) were performed using Born-Oppenheimer dynamics with the Vienna Ab-initio Simulation Package[27] (VASP), projector-augmented wave (PAW) potentials[28, 29] (500 eV cutoff), and Grimme D2 dispersion corrections.[30] *NVT* simulations were performed using a Nosé-Hoover thermostat[24, 25] with a 0.2 fs timestep. Simulations sampling slow chemistry (Approach 2) were performed using Car-Parrinello dynamics[31] with Quantum Espresso,[32] ultrasoft pseudopotentials[33] (340 eV cutoff), and with no dispersion corrections. Both the ionic and electronic degrees of freedom were coupled to a Nosé-Hoover thermostat with the electron mass and time step set to 700 au and 6.0 au (0.145 fs), respectively. All DFT and DFTB simulations performed in connection with Approach 2 had hydrogen masses replaced with deuterium ones to allow for a longer Car-Parrinello time step.

Results

Force Matching Approach 1: Fast Chemistry

An initial 1:1 water:glycine mixture was prepared with 16 molecules of each placed in a cubic 3D-periodic simulation cell at density 1.0 g cm^{-3}. DFTB with all parameters taken from mio-1-1 was used to thermalize the cell at 300 K. Isothermal isotropic compression of the cell to 2.5 g cm^{-3} was performed over 10 ps using the *NVT*/SLLOD algorithm[34, 35] and the cell was then heated with a linearly ramped thermostat to 3000 K over another 10 ps. Starting from the hot compressed state, a 10 ps DFT trajectory was integrated and 50 configurations were extracted from the last 5 ps in 100 fs intervals to force match E_{Rep} functions for the atom pairs C-C, C-N, C-O, N-O, C-H, N-H, and O-H. The force-matched DFTB model was then used to simulate a high-temperature high-pressure "cookoff" for 100 ps. The pressure was nominally constant at $\approx$50 GPa during the constant-volume cookoff. Following the cookoff, the simulation cell was adiabatically expanded to density 1.0 g cm^{-3} over 150 ps using the DOLLS algorithm.[36] The final temperature after the expansion was $\approx$1500 K.

At detonation-like conditions ($T = 3000$ K, $\rho = 2.5$ g cm^{-3}), glycine rapidly decomposes and forms a cluster of carbon, nitrogen, and oxygen. A bonding analysis was performed using both distance and lifetime criteria that reveals a systematic increase in the number of C-C bonds during the cookoff. The bonding character of carbon atoms in the cluster is predominantly sp^3. The steady formation of C-C bonds together with their sp^3 character possibly indicates the formation of diamond-like condensates. Diamond is the preferred phase at these conditions according to the phase diagram for pure carbon,[37, 38] which is also consistent with the formation of sp^3 clusters.

Figure 1 shows the evolution of the diamond-like sp^3 cluster into an sp^2 bonded sheet during adiabatic expansion. The number of carbon, nitrogen, and oxygen atoms remains nominally constant during the expansion, but a large percentage of the hydrogen atoms are lost to the surroundings to form small molecule species including water and ammonia. The loss of hydrogen is consistent with a transition from predominately sp^3 to sp^2 bonding

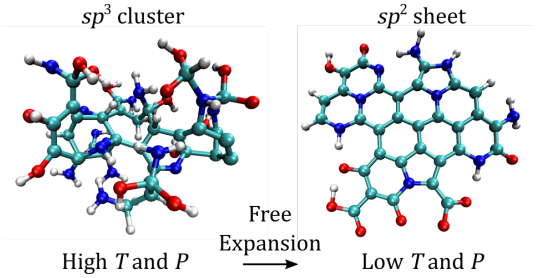

Fig. 1. At detonation conditions, glycine is predicted to decompose and form diamond-like sp^3 bonded clusters. During adiabatic free expansion, the cluster chemically rearranges into a graphitic-like sp^2 bonded sheet. Atom colors are cyan, blue, red, and white for carbon, nitrogen, oxygen, and hydrogen. Snapshots were rendered using Visual Molecular Dynamics[39] (VMD).

character for carbon atoms. The approximate state at the end of the expansion ($T \approx 1500$ K, $\rho = 1.0$ g cm^{-3}) corresponds to graphite on the phase diagram for pure carbon,[37] which is consistent with the transition to a predominately sp^2 bonded state. Soot-like products have been observed in recovered samples of shocked water:glycine mixtures.[40]

Force Matching Approach 2: Slow Chemistry

In Ref. 6 we developed a force-matched DFTB model for the initial glycine condensation reaction

$$2\mathrm{Gly} \rightarrow \mathrm{Gly}_2 + \mathrm{H}_2\mathrm{O}, \quad (5)$$

in aqueous solution at ambient conditions, which is known to be slow with a half-life on the order of years.[41] This model was shown to reproduce DFT predictions and experimental measurements for key features of the free energy surface to within a few kcal mol^{-1}. Here, our interest is to compare the validated E_{Rep} potentials generated for glycine condensation chemistry under ambient conditions to those obtained just above for extreme conditions.

Our accelerated sampling approach to generate force-matched models for slow chemical reactions was described in detail in Ref. 6, so only a brief outline is provided here. A cubic 3D-periodic simulation cell was prepared that contained two glycine molecules solvated in 55 water molecules at ($T = 300$ K, $\rho = 1.0$ g cm^{-3}). To sample otherwise rare reaction events on QMD timescales, we apply umbrella sampling[18] to bias the dynamics of collective coordinates that describe the reaction path and are coupled to the underlying atomic configurations. Specifically, glycine condensation was described with path collective coordinates $s(t)$ and $z(t)$,[14, 16] which were defined with respect to two reference configurations, namely the two glycine reactant molecules and the single diglycine product. The coordinate $s(t)$ is interpreted as measuring the distance along the path defined by the glycine and diglycine end points that are respectively mapped to $s \approx 1.1$ and $s \approx 1.9$. The coordinate $z(t)$ measures deviations from that path, which in the current application differentiates between neutral and zwitterionic charge states for the reactant and product. Additional details regarding the definitions for $s(t)$ and $z(t)$ can be found in Ref. 6.

The reaction path was sampled using 19 independent 2 ps DFT simulations, each with an applied harmonic bias potential,

$$V_{\mathrm{Bias}}(s,z) = \frac{K_s}{2}\left(s - s_{\mathrm{o}}\right)^2 + \frac{K_z}{2}\left(z - z_{\mathrm{o}}\right)^2, \quad (6)$$

acting on the path collective coordinates. Each simulation had a different s_{o}, which were set in 0.05 increments in $1.05 \leq s_{\mathrm{o}} \leq 1.95$. The z_{o} were all set to -0.10, which approximately corresponds to a path between the neutral glycine and neutral diglycine free energy minima. The force constants were set to 4000 kcal mol^{-1} and the bias potentials were applied during trajectory integration using the PLUMED 1.3 plugin.[15] Four configurations were extracted in 250 fs intervals from the first 1 ps of each independent simulation and thus collectively sample the reactants, intermediates/transients, and products.

Comparison of Force-Matched Potentials

Figure 2 shows a comparison of E_{Rep} potentials obtained from force matching to glycine chemical reactions to those from the mio-1-1 parameter set. While a repulsive potential for N-O interactions was obtained in the fit to fast chemistry (Approach 1), an analogous potential was not obtained for slow glycine condensation (Approach 2) due to inadequate sampling of those interactions. It should be noted that the cutoff distances for the two sets of force-matched models differ. In Approach 1, we set

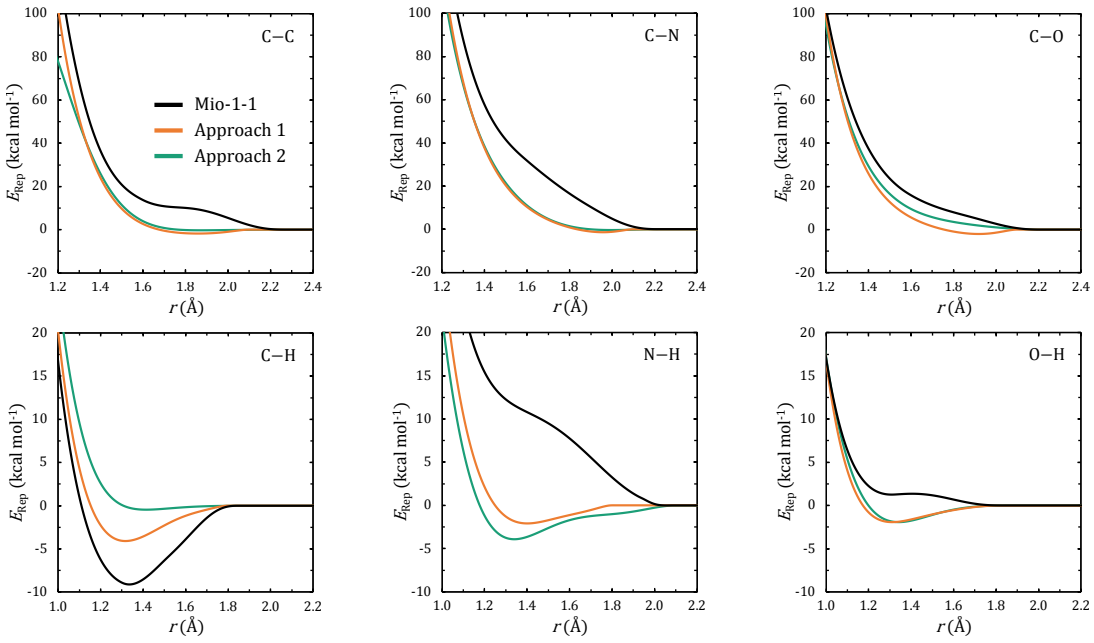

Fig. 2. Comparison of repulsive potentials from the mio-1-1 parameter set to those obtained through Approach 1 by force matching to direct high P/T DFT simulations of glycine chemistry at ($T = 3000$ K, $\rho = 2.5$ g cm^{-3}) and to those previously obtained through Approach 2 at ($T = 300$ K, $= 1.0$ g cm^{-3}).

the $r_{\mathrm{c}}^{\alpha\beta}$ to values corresponding to the first minimum in the radial distribution function for each interaction type. In Approach 2, the $r_{\mathrm{c}}^{\alpha\beta}$ were set to the mio-1-1 values. Consequently, the various E_{Rep} potentials do not all approach zero at the same value of r for a given pair type (in particular, for N-H).

It is immediately apparent that two sets of force-matched E_{Rep} potentials are more similar to each other than they are to the mio-1-1 defaults. This is despite numerous differences in the training sets generated from DFT. Those differences include the DFT code implementations (VASP vs. Quantum Espresso), the handling of core electronic states (PAW vs. ultrasoft pseudopotentials), the initial concentrations of glycine and water (1:1 vs. 2:55), the temperature and density, and the specific chemical nature of the intermediate and product configurations included in the training sets. Ascertaining which of the above factors contributes most to the differences between the two sets of force-matched E_{Rep} potentials is complicated by nonlinear dependencies and would require an extensive comparative study. However, experience suggests that differences in the training sets play the largest role in determining the quality of a force-matched potential. For instance, fitting DFTB E_{Rep} potentials to only equilibrium glycine and diglycine configurations results in a model that is unstable when taken to chemically reactive regimes.[6]

All of the force-matched E_{Rep} potentials are less repulsive than their mio-1-1 counterparts with the exception of those for the C-H pair type. The breaking and formation of C-N, C-O, N-H, and O-H bonds are explicitly sampled through the reaction path sampling used in Approach 2 whereas C-C and C-H are not. This is in contrast to the arguably better sampling of the C-C and C-H interactions under the high T/P conditions studied in Approach 1 owing both to capturing the rapid decomposition of glycine and to the significantly greater number of carbon atoms in those simulations (32 *vs.* 4). While the C-C interactions obtained in both fitting approaches are nearly the same, the C-H ones differ. In particular, the high T/P fitted C-H poten-

tial exhibits a local minimum whereas the reaction path one is purely repulsive. Both sets of fitted N-H and O-H potentials exhibit minima, which were previously correlated with an improved description of hydrogen bonding between water molecules and between water and glycine. Additional validation studies can be found in Ref. 6.

Conclusions and Conjectures

Significant similarities were found between force-matched DFTB models for glycine chemistry obtained through fitting to high temperature/pressure DFT trajectory data and through explicit reaction path sampling. One possible implication may be that force-matched DFTB models exhibit a fairly large degree of transferability over temperature, density/pressure, and composition states. This is in contrast to many classical reactive force field models and likely owes to the approximate tight-binding description of quantum mechanics that underpins the DFTB method. This similarity may also imply a certain degree of flexibility in the approach used to generate DFT training data for force matching DFTB or other semi-empirical quantum models.

In practice, generating unbiased DFT trajectories at high temperatures is significantly easier to execute than using biased dynamics approaches with collective coordinates for reaction path sampling. Thus, using high temperatures to accelerate the exploration of phase space in DFT simulations may provide for a shorter DFTB model development cycle. The reaction path fitting approach provides a clearer path to simultaneously force match DFTB models and validate them against detailed characterizations of chemical reaction free energy surfaces. Direct transference of the present results for force-matched DFTB models for glycine chemistry to other types of chemistry is not guaranteed. However, one might not unreasonably expect similar results for other organic reactions. Further comparisons between different force matched DFTB models for other condensed-phase organic reactions is warranted to ascertain both model transferability and to establish guidelines for best practices in DFTB model development.

Acknowledgments

This work was supported by NASA Astrobiology: Exobiology and Evolutionary Biology Program Element NNH14ZDA001N. This work was performed under the auspices of the U.S. Department of Energy by Lawrence Livermore National Laboratory under Contract DE-AC52-07NA27344. It has been approved for unlimited release as document LLNL-PROC-753558.

References

1. Kohn, W. and Sham, L. J., "Self-Consistent Equations Including Exchange and Correlation Effects," *Phys. Rev.*, Vol. 140, pp. A1133–A1138, 1965.

2. Elstner, M., Porezag, D., Jungnickel, G., Elsner, J., Haugk, M., Frauenheim, T., Suhai, S. and Seifert, G., "Self-Consistent-Charge Density-Functional Tight-Binding Method for Simulations of Complex Materials Properties," *Phys. Rev. B*, Vol. 58, pp. 7260–7268, 1998.

3. Qi, T., Bauschlicher, C. W., Lawson, J. W., Desai, T. G. and Reed, E. J., "Comparison of ReaxFF, DFTB, and DFT for Phenolic Pyrolysis. 1. Molecular Dynamics Simulations," *J. Phys. Chem. A*, Vol. 117, pp. 11115–11125, 2013.

4. Bauschlicher, C. W., Qi, T., Reed, E. J., Lenfant, A., Lawson, J. W. and Desai, T. G., "Comparison of ReaxFF, DFTB, and DFT for Phenolic Pyrolysis. 2. Elementary Reaction Paths," *J. Phys. Chem. A*, Vol. 117, pp. 11126–11135, 2013.

5. Goldman, N., Fried, L. E. and Koziol, L., "Using Force-Matched Potentials To Improve the Accuracy of Density Functional Tight Binding for Reactive Conditions," *J. Chem. Theory Comput.*, Vol. 11, pp. 4530–4535, 2015.

6. Kroonblawd, M. P., Pietrucci, F., Saitta, A. M. and Goldman, N., "Generating Converged Accurate Free Energy Surfaces for Chemical Reactions with a Force-Matched Semiempirical

Model," *J. Chem. Theory Comput.*, Vol. 14, pp. 2207–2218, 2018.

7. Goldman, N. and Fried, L. E., "Extending the Density Functional Tight Binding Method to Carbon Under Extreme Conditions," *J. Phys. Chem. C*, Vol. 116, p. 2198, 2012.

8. Goldman, N., Aradi, B., Lindsey, R. K. and Fried, L. E., "Development of a Multicenter Density Functional Tight Binding Model for Plutonium Surface Hydriding," *J. Chem. Theory Comput.*, Vol. 14, pp. 2652–2660, 2018.

9. Krishnapriyan, A., Yang, P., Niklasson, A. M. N. and Cawkwell, M. J., "Numerical Optimization of Density Functional Tight Binding Models: Application to Molecules Containing Carbon, Hydrogen, Nitrogen, and Oxygen," *J. Chem. Theory Comput.*, Vol. 13, pp. 6191–6200, 2017.

10. Ercolessi, F. and Adams, J. B., "Interatomic Potentials from First-Principles Calculations: The Force-Matching Method," *Europhys. Lett.*, Vol. 26, p. 583, 1994.

11. Izvekov, S., Parrinello, M., Burnham, C. J. and Voth, G. A., "Effective Force Fields for Condensed Phase Systems from Ab Initio Molecular Dynamics Simulation: A New Method for Force-Matching," *J. Chem. Phys.*, Vol. 120, pp. 10896–10913, 2004.

12. Kroonblawd, M. P. and Goldman, N., "Mechanochemical formation of heterogeneous diamond structures during rapid uniaxial compression in graphite," *Phys. Rev. B*, Vol. 97, p. 184106, 2018.

13. Laio, A. and Parrinello, M., "Escaping Free-Energy Minima," *Proc. Natl. Acad. Sci. U.S.A.*, Vol. 99, pp. 12562–12566, 2002.

14. Branduardi, D., Gervasio, F. L. and Parrinello, M., "From A to B in Free Energy Space," *J. Chem. Phys.*, Vol. 126, p. 054103, 2007.

15. Bonomi, M., Branduardi, D., Bussi, G., Camilloni, C., Provasi, D., Raiteri, P., Donadio, D., Marinelli, F., Pietrucci, F., Broglia, R. A. and Parrinello, M., "PLUMED: A Portable Plugin for Free-Energy Calculations with Molecular Dynamics," *Comput. Phys. Commun.*, Vol. 180, pp. 1961–1972, 2009.

16. Pietrucci, F. and Saitta, A. M., "Formamide Reaction Network in Gas Phase and Solution via a Unified Theoretical Approach: Toward a Reconciliation of Different Prebiotic Scenarios," *Proc. Natl. Acad. Sci.*, Vol. 112, pp. 15030–15035, 2015.

17. Zhou, Y. and Pu, J., "Reaction Path Force Matching: A New Strategy of Fitting Specific Reaction Parameters for Semiempirical Methods in Combined QM/MM Simulations," *J. Chem. Theory Comput.*, Vol. 10, pp. 3038–3054, 2014.

18. Torrie, G. M. and Valleau, J. P., "Monte Carlo Free Energy Estimates using Non-Boltzmann Sampling: Application to the Sub-Critical Lennard-Jones Fluid," *Chem. Phys. Lett.*, Vol. 28, pp. 578–581, 1974.

19. Kumar, S., Rosenberg, J. M., Bouzida, D., Swendsen, R. H. and Kollman, P. A., "The Weighted Histogram Analysis Method for Free-Energy Calculations on Biomolecules. I. The Method," *J. Comput. Chem.*, Vol. 13, pp. 1011–1021, 1992.

20. Plimpton, S., "Fast Parallel Algorithms for Short-Range Molecular Dynamics," *J. Comput. Phys.*, Vol. 117, pp. 1–19, 1995.

21. Aradi, B., Hourahine, B. and Frauenheim, T., "DFTB+, a Sparse Matrix-Based Implementation of the DFTB Method," *J. Phys. Chem. A*, Vol. 111, pp. 5678–5684, 2007, pMID: 17567110.

22. Niklasson, A. M. N., "Extended Born-Oppenheimer Molecular Dynamics," *Phys. Rev. Lett.*, Vol. 100, p. 123004, 2008.

23. Zheng, G., Niklasson, A. M. N. and Karplus, M., "Lagrangian Formulation with Dissipation of Born-Oppenheimer Molecular Dynamics using the Density-Functional Tight-Binding Method," *J. Chem. Phys.*, Vol. 135, p. 044122, 2011.

24. Nosé, S., "A Unified Formulation of the Constant Temperature Molecular Dynamics Methods," *J. Chem. Phys.*, Vol. 81, pp. 511–519, 1984.

25. Hoover, W. G., "Canonical Dynamics: Equilibrium Phase-Space Distributions," *Phys. Rev. A*, Vol. 31, pp. 1695–1697, 1985.

26. Perdew, J. P., Burke, K. and Ernzerhof, M., "Generalized Gradient Approximation Made Simple," *Phys. Rev. Lett.*, Vol. 77, pp. 3865–3868, 1996.

27. Kresse, G. and Furthmüller, J., "Efficiency of Ab-Initio Total Energy Calculations for Metals and Semiconductors using a Plane-Wave Basis Set," *Comput. Mater. Sci.*, Vol. 6, pp. 15–50, 1996.

28. Blöchl, P. E., "Projector Augmented-Wave Method," *Phys. Rev. B*, Vol. 50, pp. 17953–17979, 1994.

29. Kresse, G. and Joubert, D., "From Ultrasoft Pseudopotentials to the Projector Augmented-Wave Method," *Phys. Rev. B*, Vol. 59, pp. 1758–1775, 1999.

30. Grimme, S., "Semiempirical GGA-Type Density Functional Constructed with a Long-Range Dispersion Correction," *J. Comp. Chem.*, Vol. 27, pp. 1787–1799, 2006.

31. Car, R. and Parrinello, M., "Unified Approach for Molecular Dynamics and Density-Functional Theory," *Phys. Rev. Lett.*, Vol. 55, pp. 2471–2474, 1985.

32. Giannozzi, P., Baroni, S., Bonini, N., Calandra, M., Car, R., Cavazzoni, C., Ceresoli, D., Chiarotti, G. L., Cococcioni, M., Dabo, I., Corso, A. D., de Gironcoli, S., Fabris, S., Fratesi, G., Gebauer, R., Gerstmann, U., Gougoussis, C., Kokalj, A., Lazzeri, M., Martin-Samos, L., Marzari, N., Mauri, F., Mazzarello, R., Paolini, S., Pasquarello, A., Paulatto, L., Sbraccia, C., Scandolo, S., Sclauzero, G., Seitsonen, A. P., Smogunov, A., Umari, P. and Wentzcovitch, R. M., "QUANTUM ESPRESSO: A Modular and Open-Source Software Project for Quantum Simulations of Materials," *J. Phys. Condens. Matter*, Vol. 21, p. 395502, 2009, quantum Espresso is available at http://www.quantum-espresso.org/.

33. Vanderbilt, D., "Soft Self-Consistent Pseudopotentials in a Generalized Eigenvalue Formalism," *Phys. Rev. B*, Vol. 41, pp. 7892–7895, 1990.

34. Evans, D. J. and Morriss, G. P., "Nonlinear-Response Theory for Steady Planar Couette Flow," *Phys. Rev. A*, Vol. 30, pp. 1528–1530, 1984.

35. Daivis, P. J. and Todd, B. D., "A Simple, Direct Derivation and Proof of the Validity of the SLLOD Equations of Motion for Generalized Homogeneous Flows," *J. Chem. Phys.*, Vol. 124, p. 194103, 2006.

36. Hoover, W. G., Evans, D. J., Hickman, R. B., Ladd, A. J. C., Ashurst, W. T. and Moran, B., "Lennard-Jones Triple-Point Bulk and Shear Viscosities. Green-Kubo Theory, Hamiltonian Mechanics, and Nonequilibrium Molecular Dynamics," *Phys. Rev. A*, Vol. 22, pp. 1690–1697, 1980.

37. Wang, X., Scandolo, S. and Car, R., "Carbon Phase Diagram from Ab Initio Molecular Dynamics," *Phys. Rev. Lett.*, Vol. 95, p. 185701, 2005.

38. Correa, A. A., Bonev, S. A. and Galli, G., "Carbon under Extreme Conditions: Phase Boundaries and Electronic Properties from First-Principles Theory," *Proc. Nat. Acad. Sci.*, Vol. 103, pp. 1204–1208, 2006.

39. Humphrey, W., Dalke, A. and Schulten, K., "VMD – Visual Molecular Dynamics," *J. Mol. Graph.*, Vol. 14, pp. 33–38, 1996.

40. Sugahara, H. and Mimura, K., "Glycine Oligomerization up to Triglycine by Shock Experiments Simulating Comet Impacts," *Geochem. J.*, Vol. 48, pp. 51–62, 2014.

41. Wolfenden, R., "Benchmark Reaction Rates, the Stability of Biological Molecules in Water, and the Evolution of Catalytic Power in Enzymes," *Annu. Rev. Biochem.*, Vol. 80, pp. 645–667, 2011.